

ENHANCING SEISMIC RISK ASSESSMENT: A SPARSE MULTI-TASK LEARNING APPROACH FOR HIGH-DIMENSIONAL STRUCTURAL SYSTEMS

*SONIA ZEHSАЗ^{1A}, FARAHAZ SOLEIMANI^{1B}

¹School of Civil & Construction Engineering, Oregon State University
Kearney Hall, 1491 SW Campus Way, Corvallis, OR 97331

^Azehsazs@oregonstate.edu, <https://www.mainslab.net/>

^BFarahnaz.Soleimani@oregonstate.edu, <https://www.mainslab.net/>

Key words: Seismic Risk Assessment, Multi-Response Structures, Multi-Task Learning (MTL), Sparse Network Lasso, Seismic Demands, Engineering Demand Parameters

Abstract. Accurate quantification of engineering demand parameters is essential for probabilistic risk assessment and performance evaluation of structural systems, particularly for multi-response structures subjected to seismic events. Complex real-world structures often exhibit multiple demand parameters corresponding to distinct failure modes, necessitating a robust modeling approach that captures these interdependencies effectively. Conventional univariate models, which predict individual seismic demand responses, fail to account for the inherent correlations among multiple structural responses, leading to suboptimal predictions. Alternatively, multivariate modeling frameworks leveraging multi-task learning (MTL) techniques have emerged as a promising solution, enabling the simultaneous and joint prediction of multiple responses by improving generalization performance through the sharing of information across tasks. Despite advancements in this area, effectively capturing intricate task correlations, particularly within high-dimensional feature spaces, and mitigating the influence of noise covariance remain significant challenges. To address these challenges, this study proposes an innovative MLT framework enhanced with sparse network Lasso regularization. The proposed approach integrates MTL principles with a sparsity-inducing regularization technique through a novel penalty function that encourages highly correlated tasks to exhibit similar sparsity patterns. This integration strategically enforces sparsity in the coefficient matrix, effectively reducing the impact of irrelevant or noisy features and enhancing the resilience of the model to outliers. By leveraging this sparsity-driven regularization, the framework improves task correlation modeling and delivers precise multi-response seismic demand predictions, even in complex, high-dimensional feature spaces. As a result, the proposed framework notably advances the precision and reliability of probabilistic seismic demand analysis for multi-response structures such as bridges. By providing robust and accurate estimates of critical engineering demand parameters, it supports not only the design of new structures but also the evaluation, retrofitting, and maintenance of existing structures. This novel approach plays a crucial role across all phases of seismic hazard management, preparedness, response, repair, and recovery, by enabling informed decision-making that strengthens infrastructure resilience. Ultimately, the framework contributes to enhancing the

robustness of bridge systems against seismic hazards, safeguarding community safety, and promoting long-term infrastructure sustainability in the face of increasing natural hazard risks.

1 INTRODUCTION

Accurate and efficient joint estimation of seismic demands in multi-response structural systems is essential for robust seismic risk assessment. This need arises from the interdependent nature of engineering demand in complex infrastructure systems, such as highway bridges, where seismic performance is governed by the coupled behavior of multiple key components [1]. In these bridge systems, engineering demand parameters (EDPs), including column drifts [2], bearing and abutment deformations, and foundation rotations, serve as critical indicators of seismic vulnerability [3], [4]. Their collective response significantly influences system-level reliability [5], [6]. However, accurately predicting these EDPs within the vast, high-dimensional space of structural simulations remains a major challenge in performance-based earthquake engineering [7].

Despite advances in finite element modeling and high-performance computing, nonlinear time history analyses (NLTHAs), particularly those involving high-fidelity models, remain computationally intensive. Within the context of probabilistic seismic risk assessment, risk quantification often requires complex integrations over multidimensional probabilistic spaces that are intractable in closed form and typically necessitate large-scale Monte Carlo simulations. To alleviate this burden, surrogate demand models are widely adopted as computationally efficient approximations to NLTHAs [1].

In multi-response structural bridge systems, conventional surrogate modeling strategies typically involve constructing separate models for each EDP, depicted in Figure 1(a) [3], [8]. While this approach simplifies implementation, it becomes inefficient and laborious as model complexity increases, particularly for machine learning-based methods that require extensive calibration. More critically, such methods often fail to account for the intrinsic correlations among EDPs, potentially leading to biased or suboptimal predictions [1]. These challenges are further exacerbated by the high dimensionality of simulation inputs and the inherent uncertainties in ground motions, structural properties, and site conditions [7], [9], [10].

Neglecting these dependencies when developing frameworks not only limits the accuracy and credibility of seismic demand predictions [11] but also reduces computational efficiency. Traditional single-task (mono-task) approaches, which treat each EDP independently, may miss shared latent structures and patterns within the data, ultimately limiting scalability and generalization capabilities [12].

To address limitations of traditional models, researchers increasingly employ advanced data-driven methods. Machine learning has emerged as a powerful paradigm in structural engineering, enabling improved prediction of seismic demands by capturing complex nonlinear relationships between ground motions and structural responses [2], [13], [14], [15]. Among machine learning approaches, multi-task learning (MTL) stands out across domains for its ability to jointly learn related tasks through shared representations, as illustrated in Figure 1(b). While widely used in fields like computer vision and natural language processing, MTL remains unexplored in structural engineering, particularly for damage prediction. This highlights an opportunity to explore the potential of MTL in capturing the complex, interdependent behavior of structural systems subjected to hazard-induced demands. This approach enhances model

scalability, predictive accuracy, and generalization by enabling mutual learning across tasks [16]. Most existing models focus only on predicting point estimates of EDPs, treating multi-target learning as a simple prediction problem [1]. Such frameworks often use shared representations across tasks but fail to capture the underlying task-specific interdependencies and intrinsic correlations essential for accurate and reliable seismic demand estimation. This oversight can limit the generalization capacity of the predictive models [12].

To overcome these limitations, this study proposes an advanced MTL approach based on the Lasso framework. The proposed method incorporates task correlation into the regularization process, allowing simultaneously learning of multiple tasks. It not only captures the information about the common features of the different tasks but also preserve the supplementary information unique to each task.

In the context of seismic risk assessment for bridge systems, where EDPs are formulated as multiple prediction targets, the proposed framework unifies multi-EDP modeling into a single, efficient paradigm. By leveraging task interdependencies, it eliminates the need for separate models, significantly improving predictive performance and computational efficiency, marking a major advancement in performance-based seismic assessment.

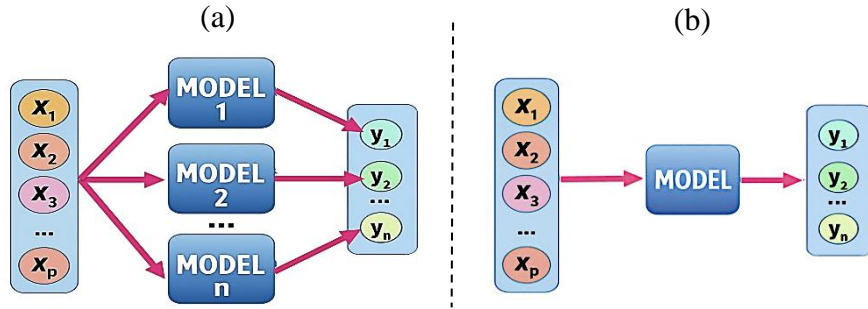


Figure 1: Conceptual Framework of Task-Based Learning Models: (a) single-task learning: independent models for individual tasks, (b) multi-task learning: shared model structure for joint task learning.

2 DESCRIPTION OF BRIDGE CHARACTERISTICS

This case study investigates the application of MTL in the probabilistic performance-based assessment of structures, focusing on the seismic behavior of tall bridge systems. Three-dimensional numerical models are developed in OpenSees [17] for representative box-girder bridges with rigid diaphragm abutments, following California bridge design standards. Bridges are classified as "tall" if their average column height exceeds 1.5 times that of regular bridges [18], [19], [20]. For each bridge type, key structural components, including superstructure, substructure, and abutments, are modeled and integrated into a global analytical framework.

The bridge deck is represented by longitudinal and transverse elastic beam-column elements, with lumped masses at nodes. Transverse elements are connected to the columns via rigid links to ensure accurate moment transfer. Columns are modeled as circular, prismatic sections using displacement-based nonlinear beam-column elements with fiber-defined cross-sections [21]. Material models include "concrete-07" for confined concrete [22], "concrete-02" for unconfined concrete [23], and "steel-02" for reinforcing steel [24], with Zero Length elements capturing isotropic strain hardening. The abutment-backfill system is modeled as a nonlinear elastic spring following Shamsabadi and Yan, calibrated based on backfill height and passive

pressure. Column-height ratios for each model were calculated relative to the average bridge height, confirming all selected bridges as “tall” under the defined criteria. Additional modeling details are available in previous work by Soleimani [20].

Table 1: The list of responses or tasks

| Regression tasks | Seismic demand | Engineering demand parameters |
|------------------|-----------------|---------------------------------------|
| y_1 (Task 1) | $\ln(\rho_c)$ | Column curvature ductility |
| y_2 (Task 2) | $\ln(\delta_d)$ | Deck displacement |
| y_3 (Task 3) | $\ln(\delta_f)$ | Foundation translational displacement |
| y_4 (Task 4) | $\ln(\theta_f)$ | Foundation rotation |
| y_5 (Task 5) | $\ln(\delta_a)$ | Active abutment displacement |
| y_6 (Task 6) | $\ln(\delta_p)$ | Passive abutment displacement |
| y_7 (Task 7) | $\ln(\delta_t)$ | Transverse abutment displacement |

Table 2: The list of input variables

| Variables | Seismic analysis characteristic | Variables | Seismic analysis characteristic |
|-----------|------------------------------------|-----------|---|
| x_1 | Soil type | x_{18} | Foundation rotational stiffness (translational direction) |
| x_2 | Girder type | x_{19} | Foundation rotational stiffness (longitudinal direction) |
| x_3 | Column cross section shape | x_{20} | Foundation translational stiffness |
| x_4 | Abutment type | x_{21} | Concrete strength |
| x_5 | Footing type | x_{22} | Reinforcement strength |
| x_6 | Fixity type | x_{23} | Mass |
| x_7 | Direction of applied ground motion | x_{24} | Damping |
| x_8 | Number of spans | x_{25} | Span ratio |
| x_9 | Span length | x_{26} | Column height ratio |
| x_{10} | Column height | x_{27} | Ground motion dt |
| x_{11} | Deck width | x_{28} | PGA |
| x_{12} | Number of cells in the box girder | x_{29} | Sa (1.0s) |
| x_{13} | Girder space | x_{30} | Sa (0.2s) |
| x_{14} | Top flange thickness | x_{31} | Sa (0.3s) |
| x_{15} | Superstructure Depth | x_{32} | Mw |
| x_{16} | Reinforcement ratio | x_{33} | R |
| x_{17} | Abutment height | x_{34} | Vs30 |

* Sa represents spectral acceleration, and Vs30 represents shear-wave velocity averaged over the 30m depth of soil

Seismic risk analysis of bridges in this study involved several key steps. First, an equal number of bridge samples and ground motions were randomly paired. The bridge models were subjected to a suite of recorded California ground motions (i.e., the Bakers 160 GM set), each containing longitudinal and orthogonal components that were randomly oriented with respect to the bridge’s longitudinal and transverse axes. To account for intensity variability, the ground motions were also applied with a scaling factor 2. Additionally, bridges were categorized into three height groups (moderately tall, very tall, and extremely tall) to systematically assess the influence of structural height on seismic response [10]. To capture modeling uncertainties, bridge samples were generated using Latin Hypercube Sampling based on the cumulative

distribution functions of the relevant structural parameters. Then, NLTHA was performed on each sample to estimate the seismic demands of the bridge components, resulting in a total of 949 recorded EDP data points. From these simulations, the peak responses of selected EDPs were extracted, which are summarized in Table 1 and used as outputs for the machine learning models. The input features, comprising structural properties and ground motion characteristics, are listed in Table 2.

3 METHODOLOGY

In high-dimensional supervised learning, regularization is key to improving generalization and interpretability. This section first introduces ℓ_1 -regularized single-task Lasso regression [25], [26], and ℓ_1/ℓ_2 -regularized multi-task extension, which promotes structured sparsity by leveraging shared information across related tasks [12], [26]. Building on this, an advanced structured multi-task Lasso-based framework is presented that integrates output dependencies through a novel penalty function, encouraging correlated tasks to select a common subset of features, thereby capturing the underlying inter-task relationships [12], [26], [27].

3.1 ℓ_1 -Regularized Single-Task Learning (STL) Regression

Consider a dataset comprising N samples, where each instance consists of a J -dimensional input vector and a corresponding K -dimensional output vector. Denote the input matrix by $\mathbf{X} = (\mathbf{x}_1, \dots, \mathbf{x}_J) \in \mathbb{R}^{N \times J}$ and the output matrix by $\mathbf{Y} = (\mathbf{y}_1, \dots, \mathbf{y}_K) \in \mathbb{R}^{N \times K}$. For each task $k = 1, \dots, K$, the output is modeled using a linear regression formulation:

$$\mathbf{y}_k = \mathbf{X}\boldsymbol{\beta}_k + \boldsymbol{\varepsilon}_k \quad (1)$$

where $\boldsymbol{\beta}_k = (\beta_{1k}, \dots, \beta_{Jk})^T \in \mathbb{R}^J$ represents the coefficient vector for task k , and $\boldsymbol{\varepsilon}_k \sim \mathcal{N}(0, \sigma^2)$ is an independent noise vector. Without loss of generality, the data are assumed to be mean-centered, i.e., $\sum_{i=1}^N y_{ik} = 0$ and $\sum_{i=1}^N x_{ij} = 0$, thus obviating the need for an intercept term.

Let $\mathbf{B} = (\boldsymbol{\beta}_1, \dots, \boldsymbol{\beta}_K)$ denote the $J \times K$ matrix of regression coefficients. The classical lasso approach estimates the optimal coefficient matrix $\hat{\mathbf{B}}^{\text{lasso}}$ by minimizing the following objective function:

$$\hat{\mathbf{B}}^{\text{lasso}} = \arg_{\mathbf{B}} \min \frac{1}{2} \|\mathbf{Y} - \mathbf{XB}\|_F^2 + \lambda \|\mathbf{B}\|_1 \quad (2)$$

where λ is a regularization parameter that controls the sparsity level, $\|\cdot\|_F$ denotes the Frobenius norm, and the mixed ℓ_1 -norm $\|\mathbf{B}\|_1 = \sum_{k=1}^K \sum_{j=1}^J |\beta_{jk}|$ encourages element-wise sparsity. While effective for isolated tasks, this approach lacks the capability to model dependencies or share features across multiple outputs.

3.2 ℓ_1/ℓ_2 -Regularized Multi-Task Learning (MTL) Regression

To incorporate structural information and leverage commonalities among tasks, MTL frameworks often use mixed-norm regularization schemes. A widely adopted approach involves the use of ℓ_1/ℓ_2 norm, which induces row-wise sparsity in the coefficient matrix \mathbf{B} , thereby facilitating joint feature selection across tasks. This formulation is particularly advantageous when a subset of predictors is hypothesized to be relevant to multiple outputs.

The optimization problem for the ℓ_1/ℓ_2 -regularized multi-task regression is defined as:

$$\hat{B}^{\ell_1/\ell_2} = \arg_B \min \frac{1}{2} \|Y - XB\|_F^2 + \lambda \|B\|_{1,2}, \quad (3)$$

where the mixed norm $\|B\|_{1,2} = \sum_{j=1}^J \|\beta^j\|_2$, β^j denotes the j -th row of B . This formulation combines the sparsity-inducing properties of the ℓ_1 -norm with the grouping effect of the ℓ_2 -norm, effectively enabling the identification of features that are jointly informative across tasks.

While the mixed norm ℓ_1/ℓ_2 regularization framework provides a principled approach for capturing shared sparsity structures, it assumes uniform relevance of features across all tasks and does not explicitly account for more intricate inter-task correlations or hierarchical dependencies.

3.3 Task-Correlation-Guided Sparse Lasso for Multi-Task Learning (MTL-TC) Regression

This section introduces an advanced framework designed to explicitly incorporate the complex dependency structure among output variables while estimating the regression coefficients. The following optimization problem is proposed:

$$\hat{B}^{TC-lasso} = \arg_B \min \frac{1}{2} \sum_{k=1}^K \|y_k - X_k \beta_k\|_2^2 + \lambda_1 \|B\|_1 + \lambda_2 D, \quad (4)$$

where the regularization term D is defined as:

$$D = \sum_{i=1}^N \sum_{k=1}^K \sum_{\substack{l=1 \\ l \neq k}}^K \frac{\|x_i^{(k)} \beta_k - x_i^{(l)} \beta_l\|_2^2}{\|x_i^{(k)} - x_i^{(l)}\|_2^2} \quad (5)$$

Here, $x_i^{(k)}$ represents the input vector for the i -th sample in task k , $\beta_k \in \mathbb{R}^J$ denotes the coefficient vector for task k . The hyperparameters λ_1 and λ_2 control the sparsity and task correlation regularization, respectively. Increasing λ_1 promotes sparsity in the coefficient matrix B by reducing the number of non-zero entries, while λ_2 encourages relatedness across tasks by penalizing differences in predictive contributions at each sample, balancing shared structures with task-specific variations. Traditional ℓ_1 -based lasso models are effective for independent sparse regression but ignore inter-task relationships, potentially leading to overfitting. Conversely, group sparsity methods (e.g., ℓ_1/ℓ_2 norm) enforce shared feature selection but can be overly restrictive, suppressing task-specific nuances. The proposed model incorporates a normalized divergence term D to strike a balance between commonality and specificity, enhancing robustness and adaptability across tasks. Optimization is performed using the L-BFGS-B algorithm, a quasi-Newton method suitable for high-dimensional, smooth, and bounded problems, allowing efficient minimization of the objective function with both sparsity and correlation regularization [28]. Hyperparameters are selected via cross-validation to ensure optimal trade-offs between sparsity, task dependency, and predictive accuracy.

4 DISCUSSION AND RESULTS

Figure 2 illustrates the complex interdependencies between structural features, seismic intensity measures, and EDPs, reinforcing the need for the proposed sparse MTL framework. Figure 2(a) shows that column curvature ductility increases with S_a (1.0s), especially for bridges with column heights between 22-27 ft. This trend suggests that higher seismic intensity leads to increased column deformations, potentially affecting structural integrity. The observed clustering and variation highlight a complex interaction that traditional single-task models may struggle to capture effectively.

A similar trend of complexity is seen in Figure 2(b), indicating that foundation rotation increases with both S_a (1.0s) and reinforcement ratio, with the latter having a stronger influence. This suggests that, beyond seismic intensity, foundation behavior is particularly sensitive to reinforcement detailing. The presence of critical outlier points further emphasizes the need to account for reinforcement design when evaluating seismic vulnerability.

Figure 2(c) extends this analysis to transverse abutment displacement, mapped as a function of span length and PGA. Higher PGA values consistently correspond to greater displacement magnitudes, while span length serves as a secondary factor that modulates the response within similar seismic conditions, revealing dynamic and bidirectional behavior under seismic loading. Notably, extreme displacement values appear under high PGA conditions, underscoring the importance of capturing these edge cases in predictive modeling.

This trend continues in Figure 2(d), which shows active abutment displacement increasing with superstructure depth and PGA with deeper superstructures exhibiting larger displacements, particularly under high PGA levels. The bidirectional displacement pattern illustrates the intricacies of abutment interaction, while the increasing variance at higher intensities indicates greater uncertainty in structural response during extreme seismic events.

Collectively, these plots reveal that seismic behavior is driven not only by seismic intensity measures such as S_a (1.0s) and PGA but also by key structural characteristics, including column height, reinforcement ratio, span length, and superstructure depth. The presence of multicollinearity between structural features and seismic inputs, for example, S_a (1.0s) correlating with column height and reinforcement ratio, while PGA aligns more with span length and depth, further complicates response prediction. Moreover, the apparent co-variation across different EDPs suggests that increases in one parameter, such as ductility, are often accompanied by increases in others, such as rotation or displacement. These insights highlight the need for a system-level modeling approach. The proposed sparse MTL framework addresses this complexity by enabling parameter sharing across correlated tasks, reducing redundancy, and improving predictive accuracy and robustness, especially in the presence of critical outliers.

Figure 3 presents a pairwise correlation analysis of EDPs, each reflecting distinct yet interrelated bridge responses to seismic loading: Column Curvature Ductility (Task 1), Deck Displacement (Task 2), Foundation Translational Displacement (Task 3), Foundation Rotation (Task 4), Active Abutment Displacement (Task 5), Passive Abutment Displacement (Task 6), and Transverse Abutment Displacement (Task 7). The matrix combines correlation coefficients (upper triangle), scatter plots with trend lines (lower triangle), and histograms (diagonal), to reveal interdependencies. Correlations range from moderate (e.g., 0.47 between Task 3 and Task 5) to near-perfect (e.g., 0.99 between Task 5 and Task 6). Deck Displacement (Task 2) demonstrates strong ties with abutment-responses: 0.74 with Task 5, 0.72 with Task 6, and 0.98

with Task 7, underscoring the role of abutment dynamics in deck performance during seismic events. Column Curvature Ductility (Task 1), while moderately correlated with Deck Displacement (0.60) and Transverse Abutment Displacement (0.59), exhibits weaker associations with other parameters, indicating it is influenced by distinct structural characteristics.

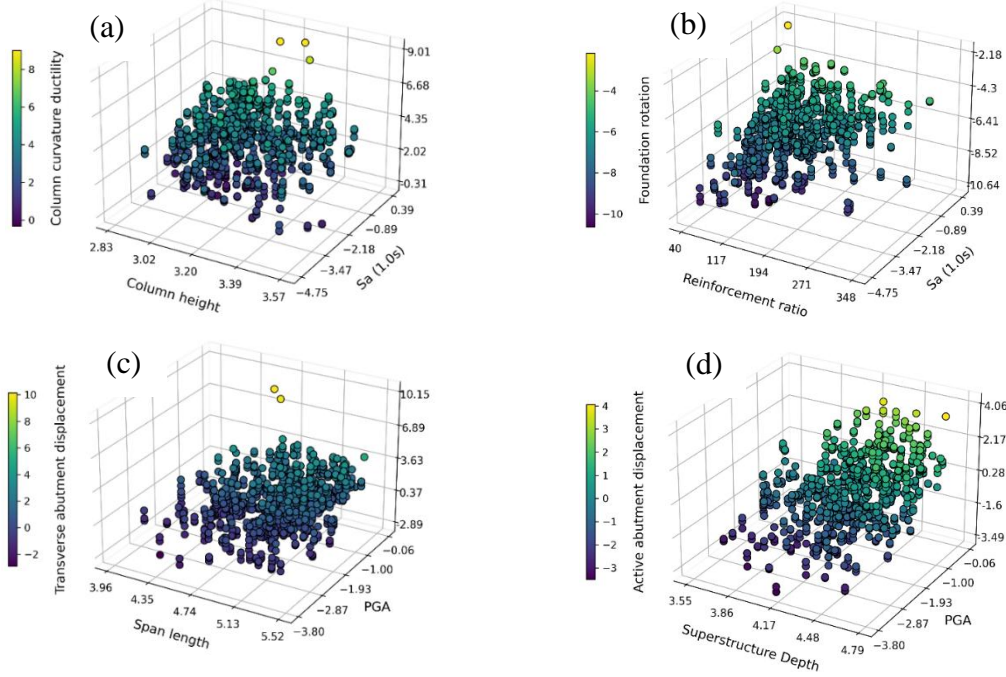


Figure 2: Variability in Bridge's Structural Seismic Demands Linked to PGA, Sa_1.0s, and Structural Characteristics

Foundation Translational Displacement (Task 3) and Rotation (Task 4) exhibit strong mutual correlation (0.67) and moderate connections with displacement tasks, reinforcing the coupled nature of foundation movements under seismic loading. Foundation Rotation also correlates with Active (0.61) and Passive (0.60) Abutment Displacements, as well as Deck (0.68) and Transverse (0.66) Abutment Displacements, underscoring its role in force transmission. A particularly strong interdependence exists between Active and Passive Abutment Displacements (0.99), indicating transverse and passive behaviors predominantly govern active abutment movements. Passive Abutment (Task 6) also correlates with Transverse Abutment (Task 7) at 0.69, though less than with Deck or Active Abutment Displacements.

The scatter plots confirm these relationships visually, with red trend lines indicating predominant positive associations. Data density and dispersion patterns, especially in moderately correlated task pairs such as Task 1 vs. Task 3 (0.47) and Task 3 vs. Task 5 (0.51), suggest complex, potentially nonlinear dependencies that may challenge single-task models. The histograms along the diagonal further illustrate the statistical diversity of each task, with some EDPs displaying symmetric distributions while others exhibit skewness. These interdependencies support the use of an MTL strategy that leverages shared information across tasks. The proposed sparse network Lasso enables selective parameter sharing for strongly

correlated tasks (e.g., Tasks 5 and 6) while preserving individual model specificity for weaker ones (e.g., Task 1). The correlation structure also reveals natural task groupings (e.g., Tasks 2, 5, 6, 7), guiding both network design and regularization. Overall, the matrix reflects the value of the proposed MTL approach in capturing complex seismic response patterns.

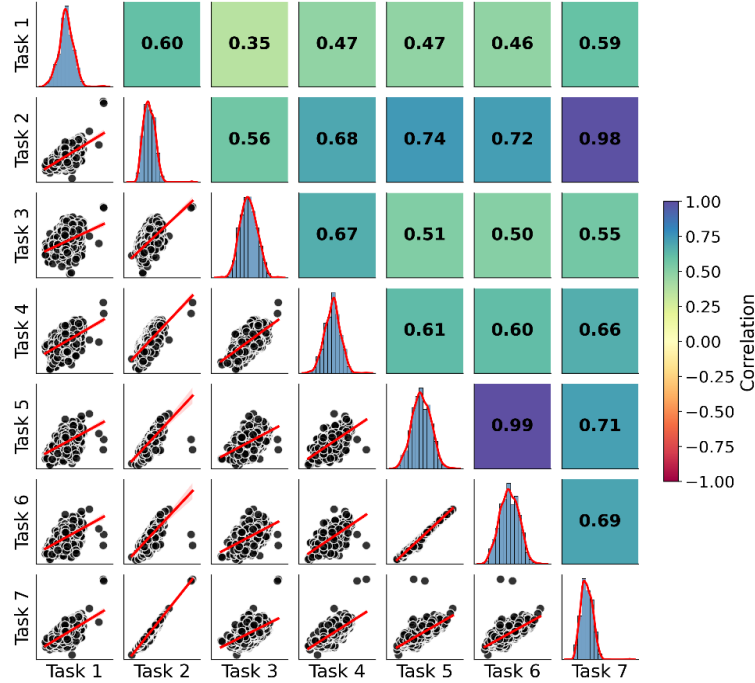


Figure 3: Correlation Matrix of Seismic Demand Tasks

Figure 4 presents a comparative evaluation of three regression methodologies (Single-Task Learning (STL), standard Multi-Task Learning (MTL), and the proposed Multi-Task Learning with Task Correlation consideration (MTL-TC)) for predicting seven EDPs in seismic bridge assessment. The ℓ_1 -regularized STL model, which treats each task independently, serves as a baseline. It yields prediction accuracies ranging from 0.63 to 0.94. STL performs well for Foundation Rotation (Task 4) and Foundation Translational Displacement (Task 3), with accuracies of 0.94 and 0.81, respectively. However, it underperforms for Deck Displacement (Task 2) and abutment-related tasks (Tasks 5–7), with accuracy values dropping to 0.63–0.66. This limitation arises from its inability to leverage shared information across tasks.

The standard MTL model, using ℓ_1/ℓ_2 regularization, enhances accuracy by enabling joint feature learning across tasks. Notable gains include a 7.5% improvement for Task 2 (from 0.66 to 0.71) and 2–3 percentage point increases for Tasks 5–7. While MTL captures shared structures more effectively than STL, it does not explicitly model inter-task correlations, which limits its full potential.

The proposed MTL-TC framework achieves the highest predictive accuracy across nearly all tasks. By combining shared feature learning with explicit task correlation modeling via sparse network Lasso regularization, it leverages both global and task-specific patterns. This dual mechanism significantly improves generalization and enhances predictive performance, especially for highly interdependent tasks. For example, Tasks 5–7 see substantial gains, with

accuracy jumping from ~ 0.65 – 0.68 (MTL) to ~ 0.88 (MTL-TC), a 20–23 percentage point increase. Task 2 also shows a strong improvement, rising from 0.71 to 0.89.

These results are consistent with the correlation patterns observed in the task dependency matrix, where Tasks 2, 5, 6, and 7 exhibited the strongest interrelationships. In contrast, Task 1 (Column Curvature Ductility) shows minimal variation across models, likely due to its relatively independent governing mechanisms. Interestingly, Task 4 (Foundation Rotation) experiences a slight dip in performance with MTL-TC, suggesting that not all tasks benefit equally from correlation-based regularization and may require specialized modeling considerations. From a practical standpoint, the MTL-TC approach offers a powerful and reliable framework for predicting critical seismic demand parameters. Its ability to effectively model complex, interdependent structural behaviors makes it a valuable tool for comprehensive seismic risk assessment in high-dimensional systems such as bridges.

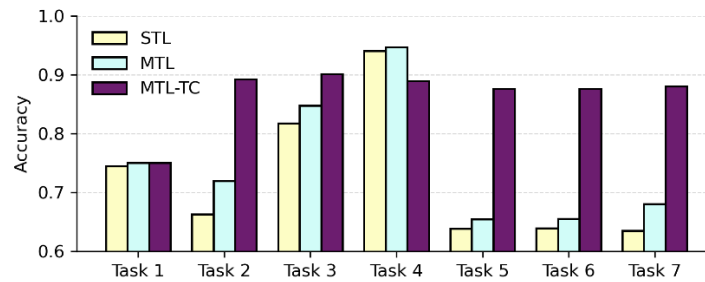


Figure 4: Prediction accuracy comparison of STL, MTL, and MTL-TC across EDPs

5 CONCLUSIONS

This study introduced a sparse MTL framework for the prediction of multiple EDPs in high-dimensional structural systems subjected to seismic loading. By explicitly modeling the intrinsic correlations among various EDPs using a network Lasso regularization, the proposed approach effectively leveraged shared information across tasks, resulting in significant improvements in prediction accuracy, especially for parameters exhibiting strong interdependence, such as abutment and deck displacements. The comprehensive analysis of parameter space, task correlation structures, and comparative model performance demonstrated that traditional single-task and standard MTL methods are limited in their ability to capture the complex, nonlinear, and correlated nature of seismic responses in bridge structures.

The results confirm that the proposed sparse MTL approach not only enhances the robustness and reliability of seismic demand predictions but also provides a scalable and interpretable modeling framework for high-dimensional risk assessment. Integrating these findings into fragility analysis improves identification of high-risk bridges and informs retrofit strategies, enhancing seismic resilience and infrastructure planning. Future work may extend this methodology to broader classes of bridges and structural systems to further improve the accuracy and applicability of seismic risk assessments.

REFERENCES

- [1] A. Du and J. E. Padgett, "Investigation of multivariate seismic surrogate demand modeling for multi-response structural systems," *Eng. Struct.*, vol. 207, p. 110210, Mar. 2020, doi: 10.1016/j.engstruct.2020.110210.
- [2] S. Zehsaz, S. Kameshwar, and F. Soleimani, "Kernel-based Column Drift Ratios Prediction in Highway Bridges," in *Proceedings of the 10th World Congress on New Technologies (NewTech '24)*, Barcelona, Spain, Aug. 2024. doi: 10.11159/icceia24.164.
- [3] B. G. Nielson, "Analytical Fragility Curves for Highway Bridges in Moderate Seismic Zones," Nov. 2005, Accessed: Sep. 21, 2024. [Online]. Available: <http://hdl.handle.net/1853/7542>
- [4] F. Soleimani, "Analytical seismic performance and sensitivity evaluation of bridges based on random decision forest framework," *Structures*, vol. 32, pp. 329–341, Aug. 2021, doi: 10.1016/j.istruc.2021.02.049.
- [5] F. Soleimani and D. Hajializadeh, "Analytical seismic resilience identifiers of bridges," in *Bridge Maintenance, Safety, Management, Digitalization and Sustainability*, CRC Press, 2024.
- [6] F. Soleimani and J. Atkins, "Natural Hazards Research Summit 2024: Neural Network Applications in Bridge Seismic Resilience Evaluation." DesignSafe-CI, Jun. 24, 2024. doi: 10.17603/ds2-de5v-ha75.
- [7] F. Soleimani and D. Hajializadeh, "State-of-the-Art Review on Probabilistic Seismic Demand Models of Bridges: Machine-Learning Application," *Infrastructures*, vol. 7, no. 5, Art. no. 5, May 2022, doi: 10.3390/infrastructures7050064.
- [8] J. Ghosh, J. E. Padgett, and L. Dueñas-Osorio, "Surrogate modeling and failure surface visualization for efficient seismic vulnerability assessment of highway bridges," *Probabilistic Eng. Mech.*, vol. 34, pp. 189–199, Oct. 2013, doi: 10.1016/j.probengmech.2013.09.003.
- [9] F. Soleimani, "Probabilistic seismic analysis of bridges through machine learning approaches," *Structures*, vol. 38, pp. 157–167, Apr. 2022, doi: 10.1016/j.istruc.2022.02.006.
- [10] F. Soleimani, "Propagation and quantification of uncertainty in the vulnerability estimation of tall concrete bridges," *Eng. Struct.*, vol. 202, p. 109812, Jan. 2020, doi: 10.1016/j.engstruct.2019.109812.
- [11] R. Rosipal and L. J. Trejo, "Kernel partial least squares regression in reproducing kernel hilbert space," *J Mach Learn Res*, vol. 2, pp. 97–123, Mar. 2002.
- [12] C. Li-na and Z. Pei-ai, "Application of Multi-task Lasso Regression in the Parametrization of Stellar Spectra," *Chin. Astron. Astrophys.*, vol. 39, no. 3, pp. 319–329, Jul. 2015, doi: 10.1016/j.chinastron.2015.07.004.
- [13] F. Soleimani and X. Liu, "Artificial neural network application in predicting probabilistic seismic demands of bridge components," *Earthq. Eng. Struct. Dyn.*, vol. 51, no. 3, pp. 612–629, 2022, doi: 10.1002/eqe.3582.
- [14] F. Soleimani and D. Hajializadeh, "Bridge seismic hazard resilience assessment with ensemble machine learning," *Structures*, vol. 38, pp. 719–732, Apr. 2022, doi: 10.1016/j.istruc.2022.02.013.

- [15] J. Atkins, F. Soleimani, and D. Hajializadeh, "Quantifying Seismic Resilience of Highway Bridges: A Case Study using Bayesian Neural Network," presented at the The 10th World Congress on New Technologies, Aug. 2024. doi: 10.11159/icceia24.136.
- [16] M. Fontana, M. Spratling, and M. Shi, "When Multi-Task Learning Meets Partial Supervision: A Computer Vision Review," Aug. 28, 2024, *arXiv*: arXiv:2307.14382. doi: 10.48550/arXiv.2307.14382.
- [17] S. Mazzoni, F. McKenna, M. H. Scott, and G. L. Fenves, *OpenSees Command Language Manual*. Pacific Earthquake Engineering Research (PEER) Center, University of California, Berkeley, 2006.
- [18] F. Soleimani, B. Vidakovic, R. Desroches, and J. Padgett, "Identification of the significant uncertain parameters in the seismic response of irregular bridges," *Eng. Struct.*, vol. 141, pp. 356–372, Jun. 2017, doi: 10.1016/j.engstruct.2017.03.017.
- [19] F. Soleimani, "Pattern Recognition of the Seismic Demands for Tall Pier Bridge Systems," *J. Earthq. Eng.*, vol. 26, no. 12, pp. 6548–6566, Sep. 2022, doi: 10.1080/13632469.2021.1927894.
- [20] F. Soleimani, "Fragility of California bridges - development of modification factors," Apr. 2017, Accessed: Apr. 22, 2025. [Online]. Available: <http://hdl.handle.net/1853/58300>
- [21] F. Soleimani, S. Mangalathu, and R. DesRoches, "A comparative analytical study on the fragility assessment of box-girder bridges with various column shapes," *Eng. Struct.*, vol. 153, pp. 460–478, Dec. 2017, doi: 10.1016/j.engstruct.2017.10.036.
- [22] J. B. Mander, M. J. N. Priestley, and R. Park, "Theoretical Stress-Strain Model for Confined Concrete," *J. Struct. Eng.*, vol. 114, no. 8, pp. 1804–1826, Aug. 1988, doi: 10.1061/(ASCE)0733-9445(1988)114:8(1804).
- [23] P. Emilio, "Method of Analysis for Cyclically Loaded R. C. Plane Frames Including Changes in Geometry and Non-Elastic Behavior of Elements under Combined Normal Force and Bending," 1973. Accessed: Apr. 22, 2025. [Online]. Available: <https://www.semanticscholar.org/paper/Method-of-Analysis-for-Cyclically-Loaded-R.-C.-in-Emilio/2a138754feb619fbe42d162428b3709d2a69672e>
- [24] F. C. Filippou, E. P. Popov, and V. V. Bertero, *Effects of Bond Deterioration on Hysteretic Behavior of Reinforced Concrete Joints*. Earthquake Engineering Research Center, University of California, 1983.
- [25] R. Tibshirani, "Regression Shrinkage and Selection Via the Lasso," *J. R. Stat. Soc. Ser. B Stat. Methodol.*, vol. 58, no. 1, pp. 267–288, Jan. 1996, doi: 10.1111/j.2517-6161.1996.tb02080.x.
- [26] X. Chen, S. Kim, Q. Lin, J. G. Carbonell, and E. P. Xing, "Graph-Structured Multi-task Regression and an Efficient Optimization Method for General Fused Lasso," May 20, 2010, *arXiv*: arXiv:1005.3579. doi: 10.48550/arXiv.1005.3579.
- [27] "GFLASSO: Graph-Guided Fused LASSO in R." Accessed: Apr. 17, 2025. [Online]. Available: <https://www.datacamp.com/tutorial/gflasso-R>
- [28] U. Kumar, "Numerical optimization based on the L-BFGS method," Towards Data Science. Accessed: Apr. 17, 2025. [Online]. Available: <https://towardsdatascience.com/numerical-optimization-based-on-the-l-bfgs-method-f6582135b0ca/>